Discontinuous Fluctuation Distribution for Time-Dependent Problems

Matthew Hubbard[1]

School of Computing, University of Leeds, Leeds, LS2 9JT, UK
meh@comp.leeds.ac.uk

1 Introduction

For some years now, the fluctuation distribution approach to approximating multidimensional systems of conservation laws has been able to produce accurate simulations of complex steady state fluid flow phenomena using unstructured meshes [DSA00]. More recent research has illustrated their potential for providing a similar level of accuracy in the simulation of time-dependent problems (see the notes in [VKI05] for a recent overview of such methods). Even so, computational simulation of compressible fluid flow problems is still dominated by the finite volume approach.

This is changing, with the emergence of the discontinuous Galerkin (DG) approach, which can be treated as a natural generalisation of the finite volume technique which accounts directly for variation of the solution within each mesh cell rather than dealing with cell-averaged values. Fluctuation distribution schemes do, however, have inherent advantages over finite volume and discontinuous Galerkin schemes, both of which use numerical fluxes across cell boundaries in the update of the dependent variables. They instead consider how the variation within each cell (loosely speaking, a generalised flux *difference*) should affect the local evolution of the dependent variable. Fluctuation distribution schemes are also typically designed to incorporate the most important underlying physical processes: making use of the fluctuation/flux difference instead of the flux provides an environment in which it is simpler to accurately model, not only genuinely multidimensional flow physics, but also source terms when these represent processes which have a natural balance with the fluxes.

Since they are essentially alternative formulations of continuous finite element methods, existing fluctuation distribution schemes are similarly restricted by the continuity imposed on the numerical solution. This can make it difficult to apply h- and p-adaptivity or construct high order schemes which are free of numerically induced oscillations. Recent research, presented in

[Hub07, Hub08], has led to the proposal of a *discontinuous* fluctuation distribution scheme, designed to overcome such problems. It provides an alternative discontinuous model to DG which avoids the construction of numerical fluxes and has been successfully used to design a second order accurate, positive algorithm (a generalisation of the PSI scheme) which can be applied to the Euler equations of gas dynamics. This paper will discuss the extension of these schemes to time-dependent problems, and present preliminary results for scalar conservation laws in one space dimension.

2 Discontinuous Fluctuation Distribution

Consider the scalar conservation law governing the evolution of an unknown quantity $u(\mathbf{x}, t)$ and given by

$$u_t + \boldsymbol{\nabla} \cdot \mathbf{f} \;=\; 0 \qquad \text{or} \qquad u_t + \boldsymbol{\lambda} \cdot \boldsymbol{\nabla} u \;=\; 0 \tag{1}$$

on a domain Ω, with boundary conditions imposed on the inflow part of $\partial\Omega$ and appropriate initial conditions. Here $\boldsymbol{\lambda} = \partial \mathbf{f}/\partial u$ defines the advection velocity associated with the conservation law (1).

These equations will be approximated by discretising an integrated form of the conservation law, assuming that the representation of u is piecewise polynomial with discontinuities allowed at the interfaces between the cells of the computational mesh. Integrating the spatial derivative terms over the whole domain gives

$$\int_\Omega \boldsymbol{\nabla} \cdot \mathbf{f} \; d\Omega \;=\; \sum_{j=1}^{N_c} \int_{C_j} \boldsymbol{\nabla} \cdot \mathbf{f} \; d\Omega \;+\; \sum_{k=1}^{N_f} \lim_{\epsilon \to 0} \int_{{F_k}^\epsilon} \boldsymbol{\nabla} \cdot \mathbf{f} \; d\Omega \,, \tag{2}$$

in which N_c, N_f are the numbers of cells and faces in the mesh, respectively, and the final term represents the integrals over the interfaces, which are being treated as limiting cases of degenerate cells whose widths (ϵ) perpendicular to the adjacent cell faces tend to zero.

Now assume that, in d space dimensions, the computational mesh cells are d-dimensional simplices, that u varies linearly with these cells, and that an appropriate (conservative) linearisation exists for the system [VKI05]. The cell spatial fluctuations can now be written

$$\phi_j \;=\; -\int_{C_j} \boldsymbol{\nabla} \cdot \mathbf{f} \; d\Omega \;=\; \oint_{\partial C_j} \mathbf{f} \cdot \mathbf{n} \; d\Gamma \;=\; -\frac{1}{2} \sum_{i \in C_j} u_i \, \widetilde{\boldsymbol{\lambda}} \cdot \mathbf{n}_i \,, \tag{3}$$

where the symbol $\widetilde{\;}$ indicates an appropriately linearised quantity. The index i loops over the vertices of the mesh cell and $\mathbf{n}_i$ is the inward unit normal to the i^{th} face (opposite the i^{th} vertex) multiplied by the length of that edge. The interface spatial fluctuations can also be evaluated exactly, giving

$$\psi_k \;=\; -\lim_{\epsilon\longrightarrow 0}\int_{{F_k}^\epsilon} \boldsymbol{\nabla}\cdot\mathbf{f}\;d\Omega\,,\; =\; \int_{F_k}[\mathbf{f}\cdot\mathbf{n}]\;d\Gamma \;=\; -\frac{1}{2}\sum_{i\in F_k}[u_i]\,\widehat{\boldsymbol{\lambda}}\cdot\mathbf{n}\,, \qquad (4)$$

where $\widehat{\boldsymbol{\lambda}}$ represents a second (different) set of conservatively averaged values, and [ ] represents the jump in a quantity across an interface (where u_i is considered to be dual-valued), the sign of the difference being dictated by the direction chosen for $\mathbf{n}$. This term is simply the integral over the interface of the flux difference across it.

Each mesh node corresponds to many cell vertices and multiple values of u. When all of the cell- and interface-based fluctuations are distributed, each u_i^j (the value associated with vertex i of cell j) can receive contributions from precisely one cell and d interfaces (subject to the application of boundary conditions). When this is combined with a simple forward Euler discretisation of the time derivative it leads to an iterative update of the form

$$(u_i^j)^{n+1} \;=\; (u_i^j)^n + \frac{(d+1)\Delta t}{S_j}\left(\alpha_i^j\phi_j + \sum_{k=1}^{d}\alpha_i^k\psi_k\right)\,, \qquad (5)$$

in which Δt is the time-step, S_j is the volume of cell j, $\alpha_i^{j/k}$ are the distribution coefficients which indicate the appropriate proportions of the fluctuations to be sent from cell j/interface k to vertex i of cell j. Conservation is assured as long as $\sum_{i\in C_j}\alpha_i^j = \sum_{i\in F_k}\alpha_i^k = 1,\ \forall j,k,$ *i.e.* the whole of each fluctuation is distributed to the cell vertices. The precise properties of the scheme depends on the choice of the distribution coefficients. In particular, the discontinuous PSI scheme described in [Hub07, Hub08] is conservative, positive for an appropriate limit on Δt, given by

$$\Delta t \;\leq\; \frac{S_j/(d+1)}{\sum_{l\in C_j}(k_l^j)^+} \qquad \forall \text{ cells } j\,, \qquad (6)$$

linearity preserving (and hence second order accurate for piecewise linear u), compact, upwind and continuous. Note that $k_l = \frac{1}{2}\boldsymbol{\lambda}\cdot\mathbf{n}_l$ are the standard inflow parameters which govern the upwinding.

2.1 Time-Dependent Problems

The development of time-dependent fluctuation distribution schemes in which u is continuous has tended to treat the time derivative in a slightly different manner to the spatial derivatives (see, for example, [AM03, RCD05]). However, for the purposes of this discussion the time dimension will be treated precisely as an additional spatial dimension, in which the solution is being advected with speed $\lambda_t = 1$. Equation (1) can now be written as

$$\boldsymbol{\nabla}^t\cdot\mathbf{f}^t \;=\; 0 \qquad \text{or} \qquad \boldsymbol{\lambda}^t\cdot\boldsymbol{\nabla}^t u \;=\; 0\,, \qquad (7)$$

in which $\boldsymbol{\nabla}^t$, $\mathbf{f}^t$ and $\boldsymbol{\lambda}^t$ have all been augmented appropriately. The discontinuous fluctuation distribution schemes outlined earlier in Section 2 can now be applied to these equations, albeit on a $d+1$-dimensional space-time mesh.

2.2 One Space Dimension

The new scheme is most easily illustrated in one space dimension. Figure 1 shows two possible configurations for the discretisation of a rectangular space time block of dimensions $\Delta x \times \Delta t$, in which it is subdivided into two triangles. The interfaces between the triangles, at which the discontinuities occur, are indicated by the dashed rectangles. The reverse configuration also illustrates the behaviour of the distribution when the flow velocity is in the opposite direction. The arrows indicate the upwind directions in which the fluctuations are distributed and, importantly, show that since $\lambda_t = 1$, upwinding always sends the fluctuations arising from the discontinuities at a fixed time level forward in time. This allows the solution to be found sequentially, stepping forward in time and solving at each time level instead of having to approximate the full space-time domain at once.

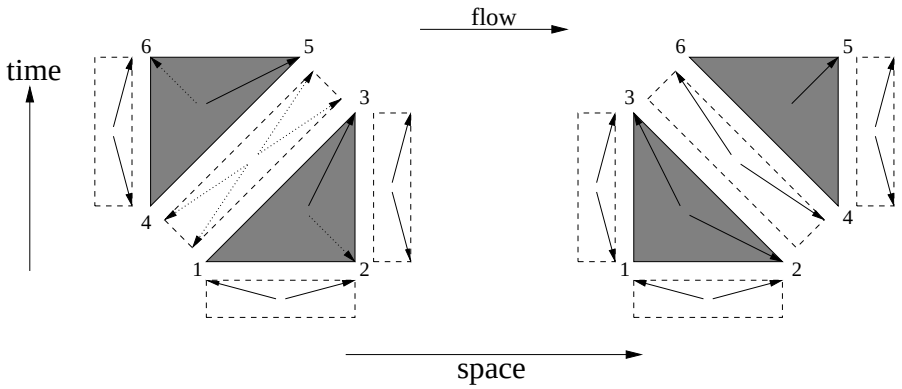

Fig. 1. Fluctuation distribution for a one-dimensional space-time block for flow from left to right (showing both orientations for the diagonal). Solid arrows show vertices to which a proportion of the fluctuation will always be distributed. Distribution indicated by the dotted arrows is dependent on the magnitude of the velocity $\boldsymbol{\lambda}$.

The system can now be approximated at the new time level by iterating the following to convergence:

$$(u_i^j)^{(m+1)} \;=\; (u_i^j)^{(m)} + \frac{2\Delta\tau}{\Delta x \Delta t}\left(\alpha_i^j \phi_j + \sum_{k=1}^{d} \alpha_i^k \psi_k\right). \tag{8}$$

The values of u_5 and u_6 (see Figure 1) form the solution at the new time level. Note that this method is positive for *any* value of Δt, though the above iteration is only positive at each stage for values of $\Delta\tau$ governed by (6).

The time derivative does not have to be treated exactly like the space derivatives. Using the approach typical of the continuous time-dependent schemes [AM03, RCD05] (which do not usually subdivide the space-time cells

into simplices) to distribute the cell fluctuations in the discontinuous case leads to a scheme which is only first order accurate. It is not yet clear why this should be so and other possibilities are being investigated to try to remove the asymmetry which appears in the mesh of simplices.

3 Numerical Results

The one-dimensional scalar advection equation was modelled, with

$$u(x,0) \;=\; \begin{cases} G(x) & \text{for } 0 \le x \le 1 \\ 0 & \text{elsewhere,} \end{cases} \tag{9}$$

being advected with a constant velocity ($\lambda = 1$) across the domain $[-1, 2]$. Periodic boundary conditions are applied and uniform space-time meshes are used to produce all of the following results. Figure 2 shows the outcomes for two initial profiles, $G(x) = \cos^2((x - 0.5)\pi)$ and $G(x) = 1$, obtained on a 151 node uniform spatial mesh with a CFL of 0.5. The effect of increasing the CFL number and reversing the advection velocity are illustrated in Figure 3. The scheme has also been applied successfully to the one-dimensional inviscid Burgers' equation.

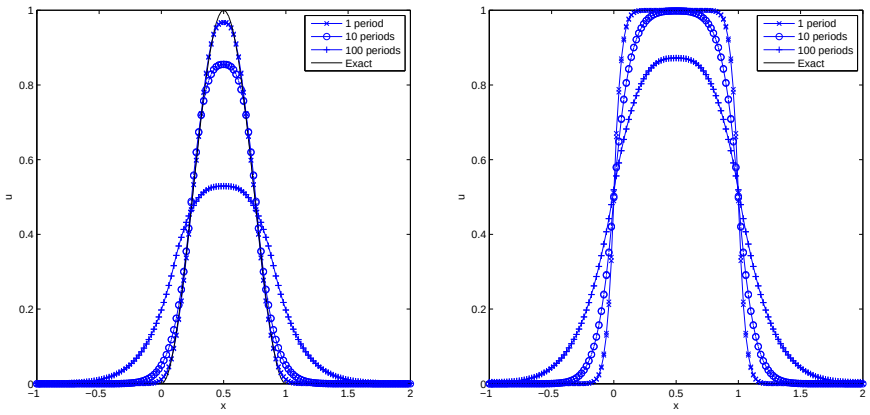

Fig. 2. Numerical approximation of the scalar advection equation for a smooth (left) and a discontinuous (right) initial profile after 1, 10 and 100 periods.

4 Summary

A framework has been proposed for the development of fluctuation distribution schemes for approximating time-dependent problems when the underlying representation of the dependent variable is allowed to be discontinuous

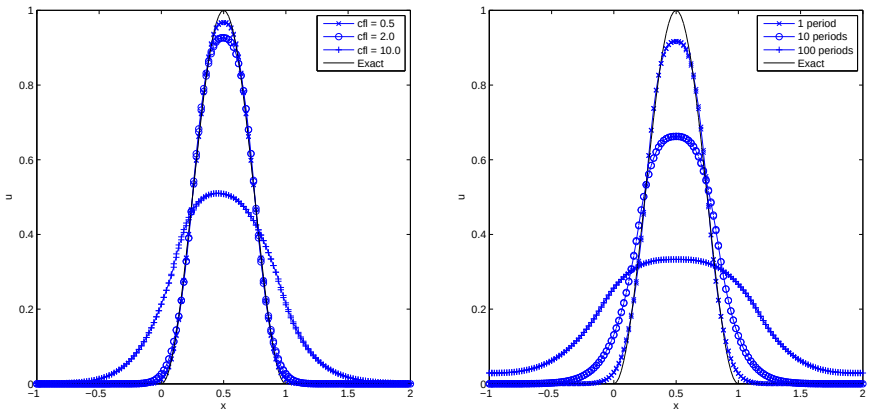

Fig. 3. Numerical approximation of the scalar advection equation for a smooth initial profile for different CFL numbers (left) and for $\lambda = -1$ (right).

across space-time mesh interfaces. It has been successfully applied to one-dimensional, scalar problems, for which second order accuracy in space and time and unconditional L^∞ stability have been verified. Further work is required to apply the approach in higher space dimensions and improve the efficiency of the approach, as well as removing the asymmetry inherent in the current space-time mesh used.

References

[AM03] Abgrall, R., Mezine, M.: Construction of second order accurate monotone and stable residual distribution schemes for unsteady flow problems. J. Comput. Phys., **188**, 16–55 (2003)

[AS08] Abgrall, R., Shu, C.-W.: Development of residual distribution schemes for the Discontinuous Galerkin methods: the scalar case with linear elements. to appear in Commun. Comput. Phys.

[DSA00] Deconinck, H., Sermeus, K., Abgrall, R.: Status of multidimensional upwind residual distribution schemes and applications in aeronautics. AIAA paper 2000–2328 (2000)

[Hub07] Hubbard, M.E.: A framework for discontinuous fluctuation splitting. Int. J. Numer. Meth. Fluids, **56**, 1505–1311 (2008)

[Hub08] Hubbard, M.E.: Discontinuous fluctuation distribution. submitted to J. Comput. Phys.

[RCD05] Ricchiuto, M., Csík, Á., Deconinck, H.: Residual distribution for general time-dependent conservation laws. J. Comput. Phys., **209**, 249–289 (2005)

[VKI05] High Order Discretization Methods. 34th Computational Fluid Dynamics course, von Karman Institute for Fluid Dynamics, Lecture Series (2005)